Peer-reviewed version available at Minerals 2019, 9, 515; doi:10.3390/min9090515

Article

The $scCO_2$ storage and sealing capacity of the Janggi Basin in Korea; based on laboratory scale experiments

Jinyoung Park[1,2], Minjune Yang[1], Seyoon Kim[1], Minhee Lee[1,*], Sookyun Wang[3]

[1] Department of Earth Environmental Sciences, Pukyong National University, Busan, Republic of Korea
[2] BK21 Plus Project of the Graduate School of Earth Environmental Hazard System, Pukyong National University, Busan, Republic of Korea
[3] Department of Energy Resources Engineering, Pukyong National University, Busan, Republic of Korea
* Correspondence: heelee@pknu.ac.kr; Tel.: +82-51-629-6630

Received: date; Accepted: date; Published: date

Abstract: Laboratory experiments were performed to measure the supercritical CO_2 ($scCO_2$) storage ratio (%) of the conglomerate and sandstone in Janggi Basin, which are classified as rock in Korea available for CO_2 storage. The $scCO_2$ storage capacity was evaluated by direct measurement of the $scCO_2$ amount replacing pore water in a reservoir rock core. The $scCO_2$ sealing capacity of the cap rock (i.e., tuff and mudstone), was also compared by measuring the initial $scCO_2$ seepage pressure (Δp) into the rock core. The measured average $scCO_2$ storage ratio of the conglomerate and the sandstone in Janggi Basin was 30.7 % and 13.1 %, respectively, suggesting that the $scCO_2$ storage capacity is greater than 360,000 metric tons in the Janggi Basin. The initial $scCO_2$ seepage pressure of the tuff in the Janggi Basin was 15 bar and continuous $scCO_2$ injection into the tuff core occurred at Δp higher than 20 bar. For the mudstone, the initial $scCO_2$ seepage pressure was higher than 150 bar (10 times higher than that of the tuff), demonstrating that the mudstone is more suitable than the tuff to shield $scCO_2$ leakage from the reservoir rock in the Janggi Basin.

Keywords: CO_2 reservoir rock; CO_2 sealing capacity; CO_2 sequestration; CO_2 storage capacity; CO_2 storage ratio; supercritical CO_2

1. Introduction

Eco-friendly plans and policies to reduce CO_2 emission are being driven forward around the world. In developed countries, CO_2 capture and sequestration (CCS) technology is partially commercialized and the total amount of subsurface CO_2 storage has been on the rise [1–4]. Since the early 2000s, the government of South Korea has been working on several projects to determine optimal CO_2 storage sites on the Korean peninsula and the Janggi Basin located in the southeastern part of the East Sea is currently being evaluated as one of the best onshore and/or offshore storage sites in Korea [5,6]. From geophysical and geological surveys, it is has become clear that the Miocene Janggi Basin consists of four small blocks (Guryongpo, Ocheon, Noeseongsan, and Yeongamri basins). The Noeseongsan block contains rudaceous sandstone and conglomerate layers considered promising for CO_2 storage sites more than 800 m deep, which also have mudstone and dacitic tuff layers above them able to serve as stable shield layers [7,8]. The Korean government has a plan to inject a hundred thousand metric tons of CO_2 in a pilot-scale onshore CO_2 storage test site in 2030 and the Janggi Basin is considered a suitable place for the $scCO_2$ storage test site. During stratigraphic analysis in 2015 and 2016, four sites in the Janggi Basin were drilled by the Korea Institute of Geoscience and Mineral Resources (KIGAM), and continuous drill cores to 1,200 m in depth were collected at each site. From the previous well logging data and the geophysical exploration results,

the area of the basin is now considered to be about 10 km^2, and it is assumed that the practical volume of the CO_2 storage formation in Janggi Basin deeper than 800 m is about 0.025 km^3 [9].

The estimation of CO_2 storage capacity of geological storage reservoirs is essential to determine reasonable CO_2 storage site candidates and is directly dependent on the practical $scCO_2$ amounts in non-aqueous phase that can be stored in the pore spaces of the reservoir rock after $scCO_2$ injection. The more water displaced by $scCO_2$ in the void spaces of the reservoir rock, the more CO_2 could be stored there. There are no exact definitions for $scCO_2$ storage capacity yet, although there are several definitions of storage capacity from previous studies [10–18]. In recent research, the $scCO_2$ storage capacity was generally defined as the proportion of the volume of $scCO_2$ stored after injection, in relation to the pore volume of the CO_2 reservoir rock [8,9]. Geological exploration and numerical simulation to determine the representative amount of $scCO_2$ that could be stored within the pore spaces of a specific reservoir formation have been major subjects in CO_2 sequestration (CS) studies. The $scCO_2$ displacement of water from pore spaces of the rock during $scCO_2$ injection can be influenced by various parameters, not only physical properties such as pore size, heterogeneity of the pore network, and injection pressure, but also mineralogical and geochemical reactivity. Thus, the best way to determine the $scCO_2$ storage amount for a specific rock formation is direct measurement of $scCO_2$ displacement of water under $scCO_2$ injection conditions. This occurs using rock cores at laboratory scale, from which the results are extended to macro scale including the entire reservoir formation [19].

The $scCO_2$ storage ratio (%) of a reservoir formation is one of the most general parameters used in laboratory work for evaluating the CO_2 storage amount of a formation [3,14]. The $scCO_2$ storage ratio is defined as that fraction of the $scCO_2$ amount occupying pore spaces after $scCO_2$ injection into a reservoir formation. It can be directly measured under $scCO_2$ injection conditions simulated at laboratory scale. The CO_2 storage capacity for a specific reservoir formation can be calculated by multiplying the $scCO_2$ storage ratio by the total void volume of the formation, ignoring the amount of dissolved CO_2. There are many benefits of direct measurement of the $scCO_2$ storage ratio because it represents the substantive amount of CO_2 retained in a specific storage formation under the $scCO_2$ injection condition. However, the number of studies on $scCO_2$ storage capacity based on direct measurement in the laboratory is very limited [9].

This study presents a novel technique by which to quantitatively measure the $scCO_2$ storage ratio under CO_2 injection conditions and to select a successful subsurface CO_2 storage test site in Korea. Laboratory experiments were performed to measure the amount of $scCO_2$ displacing water from the pore spaces of the sandstones and conglomerate cores sampled from 800–1000 m in the Janggi Basin, which is classified as an available CO_2 storage reservoir in Korea. The $scCO_2$ storage capacity of the Janggi Basin was calculated quantitatively according to the measured $scCO_2$ storage ratio and additional geophysical data.

The $scCO_2$ sealing capacity of the cap rock is another major parameter used to select successful CO_2 storage sites because it correlates to the leakage of $scCO_2$ during the anticipated duration of CO_2 sequestration. Layers of mudstone and dacitic tuff are repeated above the rudaceous sandstone and conglomerate layers in the Janggi Basin and it is considered that they can play the role of cap rocks to prevent the upward movement of $scCO_2$ from deeper reservoir rocks [21,22]. The initial seepage pressure of $scCO_2$ into the cap rock core surface, determined when the $scCO_2$ began to infiltrate the rock, was measured in the laboratory. Then, the $scCO_2$ sealing capacity of the mudstone and dacitic tuff was evaluated based on their initial $scCO_2$ seepage pressures under simulated $scCO_2$ injection P-T conditions. The change of mineralogical composition of the reservoir and cap rock after 90 days of $scCO_2$-water-rock reaction at 50 °C and 100 bar was also investigated by XRF analysis. This was done to observe the effect of $scCO_2$-related geochemical reactions on the shield capacity. From the experimental results on the $scCO_2$ storage ratio for the reservoir rock, and of the initial $scCO_2$ seepage pressure for the cap rock, the feasibility of the Janggi Basin as an available pilot-scale test site where a hundred thousand metric tons of CO_2 could be injected was evaluated. The results of this study will provide ideas for further quantitative research about the CO_2 storage capacity and CO_2 leakage safety based on practical measurements of the $scCO_2$ storage ratio and initial $scCO_2$ seepage pressure.

2. Materials and Methods

2.1. Preparation of the $scCO_2$ reservoir and capping rock cores

From the well logging data for four drilling sites in the Janggi Basin, rudaceous sandstone and conglomerate layers were considered available CO_2 storage sites and the dacitic tuff and mudstone layers overlaying them as suitable cap rock [21]. Continuous drill cores (4.2 cm average diameter) from a drilling site 1200 m deep were acquired from KIGAM. From property analysis of these cores, three rudaceous sandstone cores (JG1-S1, JG1-S2, and JG1-S3; from 930–950 m) and three conglomerate cores (JG1-C1, JG1-C2, and JG1-C3; from 950–980 m) with average porosity of 14–18 % were found and they were used for measurement of the $scCO_2$ storage ratio. For the sealing cap rock, three mudstone cores (JG1-M1, JG1-M2, and JG1-M3; from 780–790 m) and three tuff cores (JG1-T1, JG1-T2, and JG1-T3; from 800–810 m) were used for the measurement of the initial $scCO_2$ seepage pressure. Each rock core used in the experiment was cylindrical without cracks or fractures (4.2 cm diameter; length 5–7 cm). The geological map showing the area around the drilling site in the Janggi Basin and the rock cores used for the experiments are shown in Fig. 1.

The CO_2 storage and shielding capacity of rocks depend on physico-chemical properties such as porosity, permeability, reaction rate, and mineralogical stability. The porosity of the rock cores was measured using the vacuum saturation method suggested by the International Society for Rock Mechanics (ISRM) with vacuum pressure of 1 torr and vacuum time of 80 min. For each sandstone and conglomerate core, several thin slabs (1 x 1 x 0.2 cm each) were also prepared to identify the mineral composition of each core by modal analysis. To quantify the average mineral portion of each reservoir rock, 500 locations on each thin section surface of each rock slab were observed using the point counter installed in a polarizing microscope. For each mudstone and tuff core, mineralogical and geochemical analyses were performed using XRD (X-Ray Diffractometer; X'Pert-MPD, Philips, The Netherlands), and XRF (X-Ray Fluorescence Spectrometer; XRF-1800, Shimadzu, Japan) to determine their mineralogical properties.

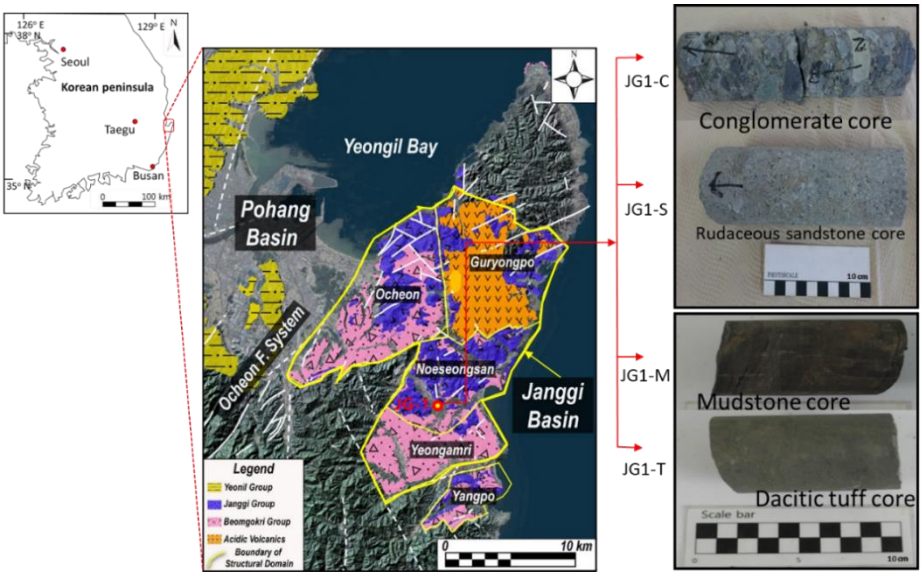

Figure 1. Geological map of the area around the drilling site (JG-1: ○) in the Janggi Basin, Korea and photographs of rock cores (right side) used for the experiment (modified from [21]).

2.2. Measurement of the $scCO_2$ storage ratio for the conglomerate and sandstone cores

When $scCO_2$ was injected, water filling the void spaces of the reservoir rock was not fully replaced by the $scCO_2$ because of the difference in interfacial tension between water and the $scCO_2$ (or difference in wettability). Thus, the amount of $scCO_2$ that could be stored in the subsurface reservoir rock is less than the total void space of the rock, and is affected by various physico-chemical parameters. For selection of an optimal CO_2 storage site, the $scCO_2$ storage capacity of rock from that specific reservoir should be estimated based on the real $scCO_2$ storage ratio. Moreover, the potential storage amount for each kind of reservoir rock should also be determined before subsurface injection of the $scCO_2$. Laboratory scale measurement of the $scCO_2$ storage ratio, displacing water from the pore spaces of Janggi sandstone and conglomerate cores under the simulated $scCO_2$ injection conditions, was performed. The experimental conditions were maintained (50 °C and 100 bar) to simulate the CO_2 storage conditions underground. The sandstone and conglomerate cores were cut (4.2 cm in diameter and 5–7 cm in length) and their surfaces were polished using powdered diamond paper. A high-pressure stainless steel cell was developed to measure the amount of $scCO_2$ stored in the pore spaces of each core after $scCO_2$ injection. It is difficult to measure the $scCO_2$ remaining in the pore space of the rock core after $scCO_2$ injection because of the leakage of the injected $scCO_2$ at the cylinder surface boundary between the cell inner wall and the rock-core wall surface. The high-pressurized cell was designed with two different walls; the inner wall was composed of a thick rubber layer (1 cm thick) and the outer wall of stainless steel. The space between the inner and the outer wall of the cell was sealed with pressurized water, which was injected from the outer part of the cell. The surface of the inner rubber wall was in tight contact with the rock core cylinder surface when the water pressure in the space was much higher than the $scCO_2$ injection pressure ($\Delta p > 100$ bar). The rock core top and bottom head surfaces were held using a screw-type steel holder with a hole in the middle for $scCO_2$ or water injection/drainage in the rock core. It was possible to shut off the bypass of injected $scCO_2$ or pore water through the boundary between the core cylinder surface and the cell inner wall, allowing the $scCO_2$ (or water) to flow only through pore spaces within the rock core. Fig. 2 shows photographs of the high- pressurized cell and the schematic diagram for the cross section of the cell used in the experiment.

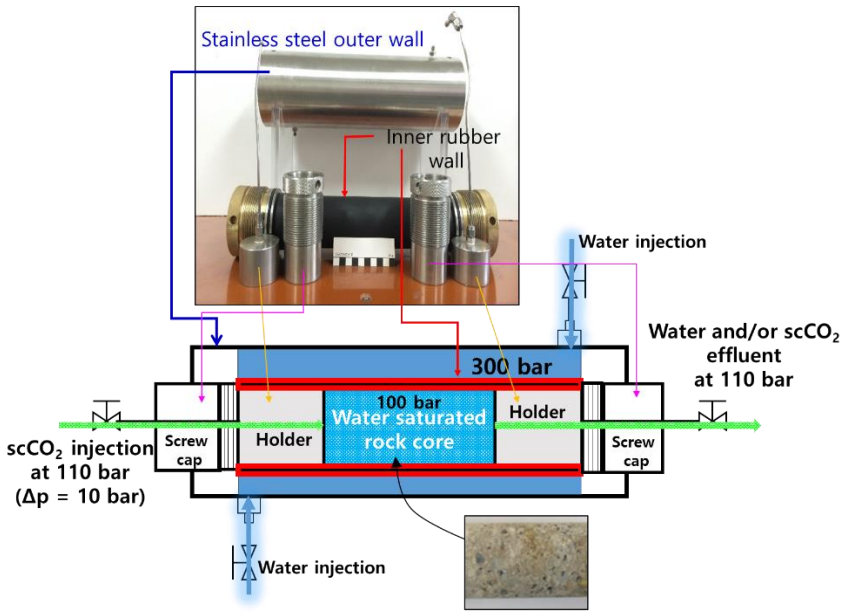

Figure 2. Photograph of the high-pressurized cell used for the experiment to measure the $scCO_2$ storage ratio.

Preprints (www.preprints.org) | NOT PEER-REVIEWED | Posted: 6 June 2019 doi:10.20944/preprints201906.0047.v1

Peer-reviewed version available at Minerals 2019, 9, 515; doi:10.3390/min9090515

For the experiment, each core was fully dried at 50 °C in an oven and then weighed. The dried core was fixed by two core holders inside the high-pressurized stainless steel cell. The outer wall of the high-pressure cell was covered by a heating jacket to maintain the cell wall at the cell temperature of 50 °C. Distilled water was injected into the sealed space between the inner wall and the outer wall of the cell by a syringe pump (Isco-D260; Teledyne Isco, Inc.), which was maintained at 300–350 bar. Then the distilled water was flushed through the core at 100 bar (the injection pressure) for three pore volumes of the core to fully saturate the core with water. Next, $scCO_2$ was injected through the influent opening to the cell to displace water from the pore spaces of the core at 110 bar (Δp = 10 bar) while more than two pore volumes of $scCO_2$ were flushed from the core (assuming that displacement of water by the $scCO_2$ was successful). All of the effluent water was stored in a small stainless storage cell and its mass was weighed to measure the amount of water displaced by the $scCO_2$ in the rock core. The high- pressurized stainless chamber (5 L capacity) was connected to the effluent of the cell to consider the boundary condition of the reservoir rock when the $scCO_2$ was flushed from the rock core in the experiment. The water in the pores was compressed as the pore pressure increased due to $scCO_2$ injection and enough water and/or $scCO_2$ volume should be provided in the chamber for the replacement of all the $scCO_2$ during the experiment. All of the high-pressurized cells were maintained at 50 °C and 110 bar after the CO_2 injection to simulate the subsurface CO_2 storage conditions. Fig. 3 shows the procedure of the experiment for $scCO_2$ exchange in the rock core.

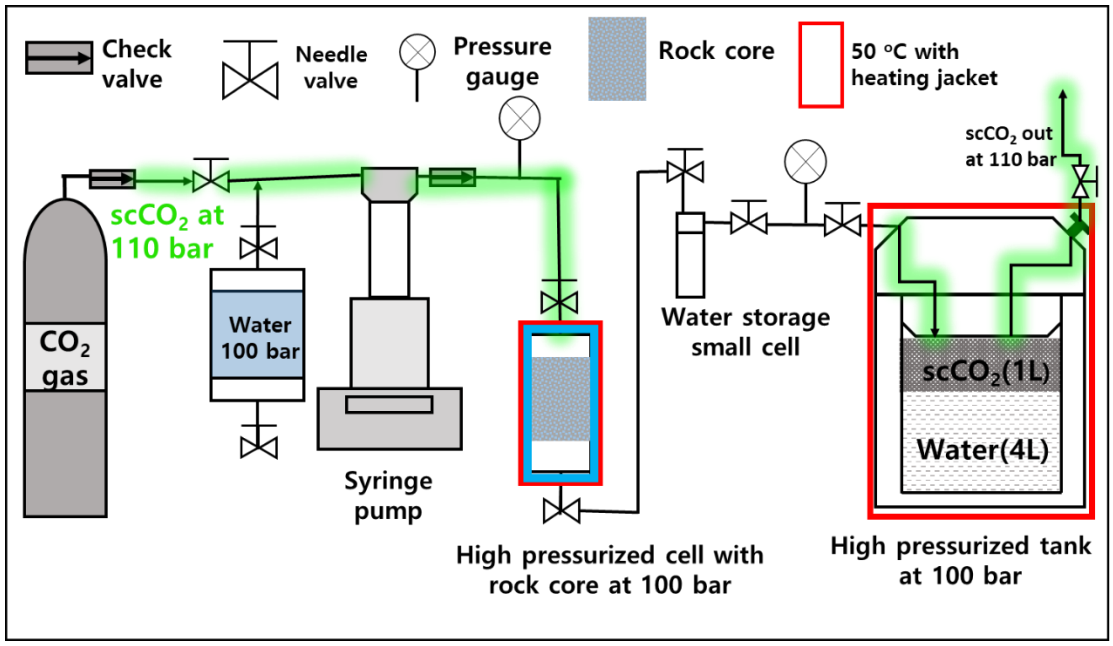

Figure 3. Schematic of the experiment to measure the $scCO_2$ storage ratio.

When the amount of water drained from the core was measured, the $scCO_2$ storage ratio for the specific rock core under the $scCO_2$ injection condition (in this case, 100 bar and 50 °C) could be calculated using equation (1).

$$\text{The } scCO_2 \text{ storage ratio (\%) } for\ the\ rock = \left(1 - \frac{W_{s-} - W_{out}}{W_s}\right) \times 100 \quad (1)$$

where W_s is the volume of water saturating the core and W_{out} is the water volume displaced by $scCO_2$ during the $scCO_2$ injection.

From equation (1), the $scCO_2$ storage capacity of the conglomerate and the sandstone formations in the Janggi Basin were estimated via equation (2) with the volume of the stratum, the average porosity, the specific gravity of the $scCO_2$, and the storage ratio of $scCO_2$ [3,14].

$$The\ storage\ capacity\ (ton) = \sum(V \times \varphi \times \rho \times \epsilon) \quad (2)$$

where V is the volume of the conglomerate or sandstone layer (estimated from the previous geological survey data), φ is the average porosity, ρ is the specific gravity of the $scCO_2$, and ε is the $scCO_2$ storage ratio. The feasibility of the Janggi Basin as a CO_2 reservoir formation was evaluated based on the $scCO_2$ storage capacity of rudaceous sandstone and conglomerate drill core samples from the Janggi Basin (total of six cores).

2. 3. Measurement of the initial $scCO_2$ seepage pressure for mudstone and dacitic tuff

When $scCO_2$ is injected into reservoir rock, it is distributed as a separate phase from water in pore spaces and begins to move slowly upward from the lower part of the reservoir rock due to buoyant force because of its lower density compared to water. Some of the injected $scCO_2$ may reach the boundary between the cap rock and the reservoir rock during continuous injection. At the early stage of $scCO_2$ injection, the amount of $scCO_2$ reaching the boundary is not much and the cap rock can prevent the intrusion of $scCO_2$ because of its low permeability. As the amount of $scCO_2$ at the boundary and its buoyant pressure increase because of continuous $scCO_2$ injection, advective and/or the diffusive intrusion of $scCO_2$ into the cap rock occurs. This pressure initiates seepage of the $scCO_2$ from the reservoir rock, threatening the leakage safety of the CO_2 storage site. The sealing capacity of the cap rock is directly dependent on the initial $scCO_2$ seepage (or intrusion) pressure on the cap rock surface [22]. The direct measurement of the initial $scCO_2$ seepage pressure of the cap rock was performed at laboratory scale to evaluate the $scCO_2$ shielding capacity of the cap rocks in the study area. The mudstone and dacitic tuff rock cores sampled during the deep drilling expedition (from 700–800 m) at the onshore site in the Janggi Basin were used for the experiment (Fig. 1).

Rock cores without cracks or fractures were cut (4.2 cm diameter, 5-6 cm length) and were then fully dried at 50 °C in an oven. Each rock core was fixed in the high-pressurized stainless steel cell (which was used in the same way as in the previous experiment, Section 2.2). Each core was saturated with distilled water at 100 bar of pore water pressure. The effluent of the cell was connected to a large tank filled with 3 L of water and 2 L of $scCO_2$ at 100 bar and 50 °C, simulating the subsurface $scCO_2$ injection conditions. The initial $scCO_2$ seepage pressure into the rock core head (higher than 100 bar: Δp = injection pressure − 100 bar), was controlled at the influent port with the regulator of the core holder in the cell bottom until the $scCO_2$ begin to penetrate the rock. The $scCO_2$ injection pressure was set 110 bar and the injection pressure was increased by 10 bar until the $scCO_2$ began to penetrate the rock core head. At the outset, the $scCO_2$ injection pressure on the core head surface was set at 110 bar (Δp = 10 bar) and any $scCO_2$ intrusion into the core was observed for 10 days. If no $scCO_2$ intrusion occurred, the injection pressure was increased by 10 bar for 10 more days to monitor any $scCO_2$ intrusion into the core. This process was repeated until the $scCO_2$ began to penetrate the rock core head. When the $scCO_2$ begin to intrude and the $scCO_2$ injection pressure started to decrease, the $scCO_2$ injection pressure was maintained until $scCO_2$ was flushed from the end of the rock core. This pressure was regarded as the initial $scCO_2$ seepage pressure (Δp) of the rock core. The $scCO_2$ shield capacity of each kind of cap rock core (dacitic tuffs and mudstones here) was evaluated by comparing their initial $scCO_2$ seepage pressures (Δp).

The mineralogical changes of mudstone and tuff were also measured to evaluate their geochemical stability for 90 days of the $scCO_2$-water-rock reaction under CO_2 storage conditions (100 bar and 50 °C). The rock core was pulverized using a mortar and ten grams of powered rock materials were mixed with 100 mL of distilled water in the high-pressurized stainless steel cell (capacity of 150 mL), of which the inner wall was coated with a Teflon layer. The void spaces in the cell were filled with $scCO_2$ using a syringe pump. Then $scCO_2$-water-rock reactions were allowed to occur in the cell at 100 bar and 50 °C, simulating the subsurface storage conditions. The total reaction time was 90 days and XRD analysis was conducted before and after the reaction to identify any mineralogical changes of the cap rock due to the $scCO_2$-water-rock reaction.

3. Results and discussion

3.1. Measurement of the $scCO_2$ storage ratio for the conglomerate and sandstone cores

Results of the modal analyses for the rudaceous sandstone and conglomerate cores are shown in Table 1 and the photomicrographs of their thin sections are shown in Fig. 4. The conglomerate was mostly composed of rhyrolitic and andesitic rock fragments (average 74.5 %), followed by quartz, clay/accessory minerals, feldspar, micas, and calcite (in descending order). The sandstone mainly consisted of quartz, rock fragments, clay/accessory minerals, feldspar, micas, and calcite. Their average proportions were 32.5 %, 23.8 %, 18.3 %, 19.4 %, 2.5 %, and 2.5 %, respectively (Table 1). From previous studies, calcite, feldspars, chlorite, micas, and clay minerals bearing Ca and Mg may control the geochemical reactions with CO_2 in the storage site, thereby regulating the physical properties of the reservoir rock [23–26]. The results from XRD analyses (not shown in this paper), showed mineral composition similar to that indicated by modal analysis.

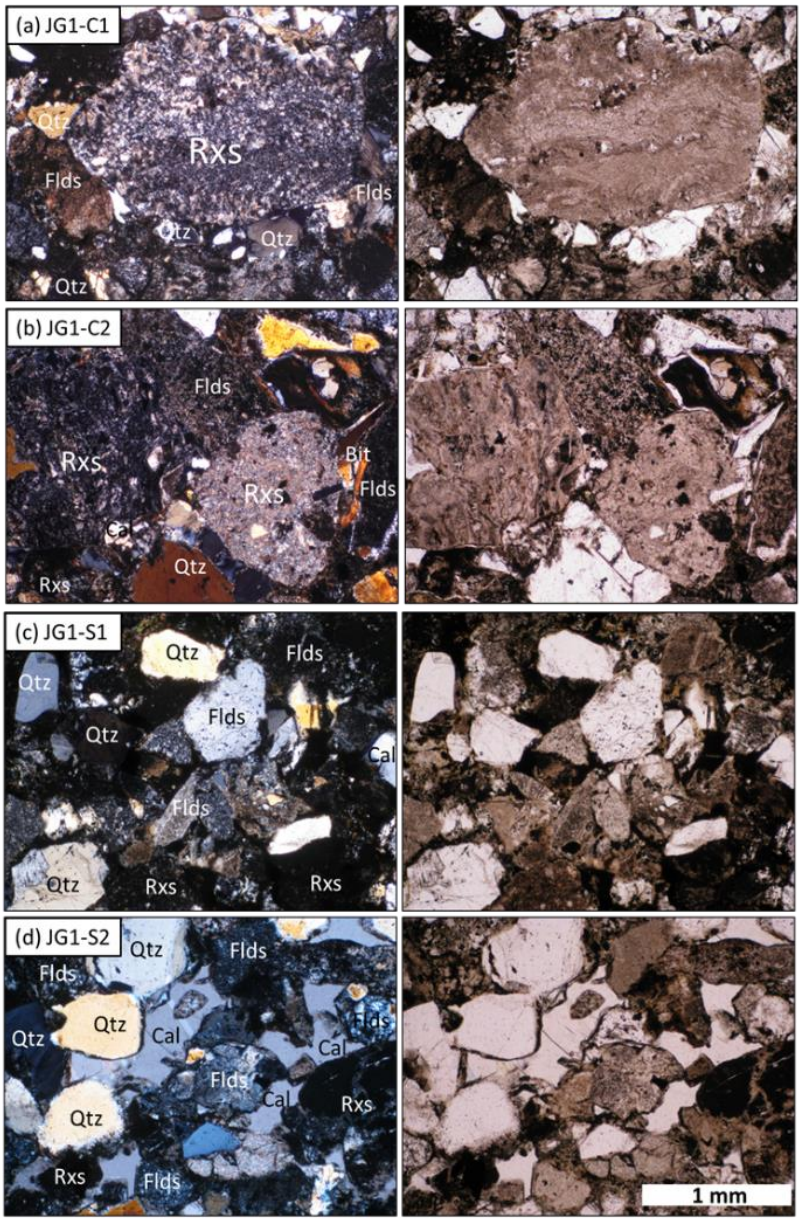

Figure 4. Photomicrographs of thin sections of the conglomerate (a and b) and the rudaceous sandstone (c and d); Left column: closed mode and right column: open mode; Qtz: quartz, Flds: feldspars, Cal: calcite, Bit: biotite, and Rxs: rock fragments.

Table 1. Petrographic detrital modal analysis of the rock cores

Rock type	Mineral portion (%)							
	Quartz	K-feldspar	Plagioclase	Rock fragment	Fine matrix and clay	Calcite	Micas	Others
JG1-C1	7.8	1.8	1.2	80.6	8.0	0.2	0.0	0.4
JG1-C2	17.8	6.6	4.8	57.4	10.8	0.4	1.2	1.0
JG1-C3	6.4	1.8	1.0	85.4	3.8	0.4	0.4	0.8
Average± standard deviation	10.7 ±6.2	3.4 ±2.8	2.3 ±2.1	74.5 ±15.0	7.5 ±3.5	0.3 ±0.1	0.5 ±0.6	0.7 ±0.3
JG1-S1	33.6	8.8	12.0	24.8	16.0	2.2	1.2	1.4
JG1-S2	31.6	11.6	8.2	24.2	18.4	0.6	4.4	1.0
JG1-S3	32.2	10.4	7.0	22.4	20.4	4.6	1.8	1.2
Average± standard deviation	32.5 ±1.0	10.3 ±1.4	9.1 ±2.6	23.8 ±1.2	18.3 ±2.2	2.5 ±2.0	2.5 ±1.7	1.2 ±0.2
JG1-M1	40.8	3.0	1.4	0.4	47.4	1.2	2.6	3.2
JG1-M2	43.8	2.8	0.6	0.0	47.4	0.4	2.4	2.6
JG1-M3	33.6	2.4	0.4	0.2	58.6	0.2	2.2	2.4
Average± standard deviation	39.4 ±5.2	2.7 ±0.3	0.8 ±0.5	0.2 ±0.2	51.1 ±6.5	0.6 ±0.5	2.4 ±0.2	2.7 ±0.4
JG1-T1	26.0	12.2	11.6	18.6	19.6	1.4	3.8	6.8
JG1-T2	19.4	10.4	14.8	11.6	32.4	1.2	4.2	6.0
JG1-T3	24.5	9.7	13.2	16.7	22.0	2.4	3.1	8.4
Average± standard deviation	23.3 ±3.5	10.8 ±1.3	13.2 ±1.6	15.6 ±3.6	24.7 ±6.8	1.7 ±0.6	3.7 ±0.6	7.1 ±1.2

* JG1-C: conglomerate cores; JG1-S: rudaceous sandstone cores, JG1-M: mudstone cores and JG1-T: dacitic tuff cores.

The porosity of the conglomerate and the sandstone cores were measured and are shown in Table 2. The average porosity of the conglomerate and the rudaceous sandstone was 17.8 % and 14.5 %, respectively, suggesting that they fall within the porosity range of typical CO_2 storage formations in other places, where large amounts of $scCO_2$ have been injected [20,27–32]. At 110 bar of the initial $scCO_2$ injection pressure condition (Δp = 10 bar between the injection pressure and the pore water pressure in the core), $scCO_2$ intruded into the rock core fixed in the cell and began to displace water from the pore spaces of the core. More than two pore volumes of $scCO_2$ was flushed out from the core at 110 bar (Δp = 10 bar). Then the $scCO_2$ storage ratio of each conglomerate and sandstone core was measured and their averages are shown in Table 2. The calculated average $scCO_2$ storage ratio of the Janggi conglomerates was 30.7 %, suggesting that 30.7 % of the void space in the conglomerate was

filled with $scCO_2$ while the pressure difference between the $scCO_2$ injection and the pore water was maintained at 10 bar. The average $scCO_2$ storage ratio of rudaceous sandstones was 13.0 %, which was about two-fifths that of the conglomerate. From these results, both kinds of rock had great capability for storing CO_2 in their pore spaces, but the conglomerate was considered a better option for the CO_2 storage site than was the rudaceous sandstone.

The $scCO_2$ storage ratio values were used for the estimation of the CO_2 storage capacity for the Janggi Basin (Table 3). From previous studies [21], it was known that the Janggi Basin extends horizontally over about 0.25 km^2 below the depth of 800 m and that the thickness of both the conglomerate and sandstone layers available for the CO_2 reservoir was 100 m (about 1:1 ratio), assuming that the maximum volume of the CO_2 storage formation in the Janggi Basin under 800 m in depth is about 0.025 km^3. The parameter values used to calculate the CO_2 storage capacity and the calculated $scCO_2$ capacity for the two formations are shown in Table 3. The $scCO_2$ storage capacity of the reservoir rocks around the probable $scCO_2$ injection site in Janggi Basin was calculated to be 368,742 metric tons, demonstrating that the conglomerate and sandstone formations in Janggi Basin have great potential for use as a pilot test site for CO_2 storage in Korea (to receive more than 100,000 metric tons of CO_2 injection at the test storage site).

Table 2. The $scCO_2$ storage ratios of conglomerate and rudaceous sandstone cores at the Janggi Basin

Core number	Rock type	Porosity (%)	The $scCO_2$ storage ratio (%)
JG1-C1	Conglomerate	19.23	23.56
JG1-C2		18.92	35.41
JG1-C3		15.12	31.20
Average		17.76	30.72
JG1-S1	Rudaceous sandstone	10.54	13.12
JG1-S2		16.44	16.28
JG1-S3		17.26	9.64
Average		14.75	13.01

Table 3. The $scCO_2$ storage capacity of conglomerate and rudaceous formations at the Janggi Basin (unit: metric ton)

Rock type	The calculated $scCO_2$ storage amount for conglomerate and rudaceous formation (metric ton)
Coglomerate	V(50m x 250m x 1000m) x φ(0.1776) x ρ*(400 kg/m^3) x ε(0.3072) = 272,793.6
Rudaceous sandstone	V(50m x 250m x 1000m) x φ(0.1475) x ρ*(400 kg/m^3) x ε(0.1301) = 95948.8

* Density of $scCO_2$ at 100 bar and 50 °C (from [33,34])

3.2. Measurement of the initial $scCO_2$ seepage pressure for mudstone and dacitic tuff

The mineralogical changes of the mudstone and the dacitic tuff after 90 days of $scCO_2$-water-rock reaction were investigated by XRF analyses and their results are shown in Table 4. The results indicated that even after 90 days of reaction, the proportions of the major constituents of the two kinds of rock were not significantly changed except for a minor decrease of SiO_2 and CaO. These originated from increased dissolution of calcite, Ca-feldspar, and Ca-bearing silicates (Table 4). It is

suggested that the mudstone and the dacitic tuff in the Janggi Basin is likely to maintain significant stability against $scCO_2$-involved geochemical reactions during CO_2 storage.

Table 4. XRF analysis of mudstone and dacitic tuff before and after 90 days of $scCO_2$-water-rock reaction

Composition	Ratio (wt%)					
	JG1-M1		JG1-M2		JG1-T1	
	Before	After 90 day reaction	Before	After 90 day reaction	Before	After 90 day reaction
SiO_2	**57.2**	**56.51**	**56.36**	**55.65**	**57.28**	**56.76**
Al_2O_3	20.84	20.89	17.88	17.94	18.54	18.69
TiO2	0.78	0.78	0.62	0.62	0.79	0.76
Fe_2O_3	5.32	5.29	4.99	5.06	8.06	8.19
MnO	0.09	0.08	0.12	0.12	0.20	0.19
MgO	0.79	0.92	0.71	0.81	2.02	1.98
CaO	**1.14**	**1.08**	**1.16**	**1.09**	**4.27**	**3.61**
Na_2O	1.63	1.73	1.32	1.36	2.98	3.00
K_2O	2.30	2.40	2.04	2.09	1.15	1.04
P_2O_5	0.09	0.09	0.15	0.15	0.19	0.19
LOI	9.61	10.07	14.44	14.96	4.37	5.23
Total	99.8	99.85	99.79	99.85	99.84	99.87

Results from the measurement of the initial $scCO_2$ seepage pressure (Δp) for the mudstone and the tuff core are shown in Fig. 5. For all of the tuff cores, the $scCO_2$ began to intrude into the rock core at 115 bar (Δp = 15 bar) and continuous $scCO_2$ injection into the core occurred at Δp higher than 20 bar. This suggests that the initial $scCO_2$ seepage pressure (Δp) of the dacitic tuff ranged from 15 to 20 bar under the conditions of 100 bar and 50 °C. In the tuff cores, 8–10 % of the void space (0.7–0.9 mL) was filled by $scCO_2$ at Δp higher than 20 bar. In a previous study (Kim et al. 2019), the average initial $scCO_2$ seepage pressure of the sandstone and conglomerate in the Janggi Basin was lower than 10 bar (mostly < 5 bar), which was less than one-third that for the dacitic tuff. For the mudstone cores in the Janggi Basin, the $scCO_2$ did not penetrate the core surface and the stored $scCO_2$ was less than 0.005 mL even when the injection pressure was 250 bar (Δp = 150 bar) for 30 days. This suggests that the initial $scCO_2$ seepage pressure for the mudstone core was much higher than 150 bar (10 times higher than for the tuff). Based on the initial $scCO_2$ seepage pressure, the mudstone formation in Janggi Basin was much more suitable than the tuff formation as a shield to $scCO_2$ leakage from the reservoir rock.

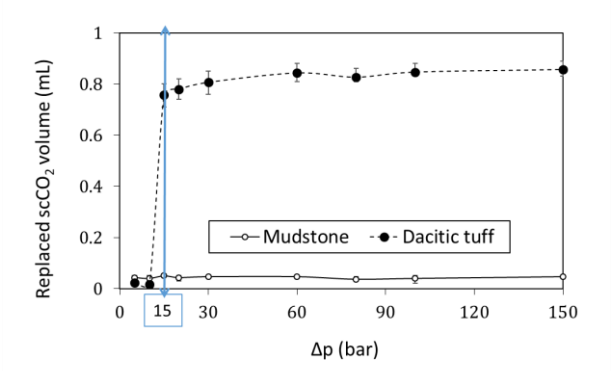

Fig. 5. Initial $scCO_2$ seepage pressure (Δp) and the volume of $scCO_2$ stored in mudstone and dacitic tuff cores.

4. Conclusions

One of the main issues for the geological sequestration of CO_2 has been how to determine an optimal storage site and what the main parameters for consideration should be. During the last two decades, evaluation of the storage capacity and the leakage safety has been considered essential for optimal storage site selection. However, only rough estimations were made of the reservoir and the capping rock using conventional parameters such as porosity and permeability, and/or by using large-scale information acquired from geophysical exploration and geological field observation. The quantitative evaluation of CO_2 storage capacity and of the risk of CO_2 leakage has been very limited even at laboratory scale. This study presents an easy and effective technique by which to evaluate the CO_2 capacity of reservoir rock and the leakage safety of the cap rock for a specific CO_2 storage site.

The scale-up estimation of the CO_2 storage capacity for the conglomerate and the rudaceous sandstone in the Janggi Basin of Korea was performed based on direct measurement of the $scCO_2$ storage ratio. The safety risk of $scCO_2$ leakage for cap rock of dacitic tuff and mudstone in the Janggi Basin was also quantitatively evaluated by measuring the initial $scCO_2$ seepage pressure. The experimental results successfully demonstrated that the conglomerate and sandstone formations of the Janggi Basin are suitable as a geological storage test site for injection of a hundred thousand tons of CO_2. It was also verified that the mudstone formation in the Janggi Basin is adequate to prevent the seepage of buoyant $scCO_2$ from the reservoir site because its high initial seepage pressure (difference between the pore water pressure of the mudstone and the $scCO_2$ injection pressure: Δp) was higher than 150 bar. The quantitative measurement of the $scCO_2$ storage ratio and the initial $scCO_2$ seepage pressure applied in this study can be used to determine practicable CO_2 storage sites and could also provide meaningful information for future decisions regarding $scCO_2$ injection conditions.

Acknowledgments: This research was supported by a grant (16CTAP-C115166-01) from the Technology Advancement Research Program (TARP) funded by the Ministry of Land, Infrastructure, and Transport of the Korean government. The authors would like to express their gratitude to the anonymous reviewers for their critical comments and advice.

Author Contributions: Minhee Lee and Jinyoung Park conceived and designed the methodology and the experiments; Jinyoung Park , Minhee Lee and Seyoon Kim performed the experiments and the data analyses; Sookyun Wang and Minjune Yang contributed materials and data interpretation; Minhee Lee wrote the paper to prepare the submission.

Conflicts of Interest: The authors declare no conflict of interest.

References

1. Michael, K.; Golab, A.; Shulakova, V.; Ennis-King, J.; Allinson, G.; Sharma, S.; Aiken, T. Geological storage of CO_2 in saline aquifers-A review of the experience from existing storage operations. *Int. J. Greenh. Gas Control* **2010**, *4*, 659–667, doi:10.1016/j.ijggc.2009.12.011.

2. Leung, D.Y.C.; Caramanna, G.; Maroto-Valer, M.M. An overview of current status of carbon dioxide capture and storage technologies. *Renew. Sustain. Energy Rev.* **2014**, *39*, 426–443, doi:10.1016/j.rser.2014.07.093.

3. Bachu, S. Review of CO_2 storage efficiency in deep saline aquifers. *Int. J. Greenh. Gas Control* **2015**, *40*, 188–202, doi:10.1016/j.ijggc.2015.01.007.

4. IPCC IPCC special report on the impacts of global warming of 1.5 °C above pre-industrial levels and related global greenhouse gas emission pathways. In: The Context of Strengthening the Global Response to the Threat of Climate Change, Sustainable Development, and Efforts to Eradicate Poverty. **2018**.

5. Kim, M.-C.; Kim, J.-S.; Jung, S.; Son, M.; Sohn, Y.K. Bimodal volcanism and classification of the Miocene basin fill in the northern area of the Janggi-myeon, Pohang, Southeast Korea. *J. Geol. Soc. Korea* **2011**, *47*, 585–612.

6. Song, C.W. A study on potential geologic facility sites for carbon dioxide storage in the Miocene Pohang Basin, SE Korea. *J. Geol. Soc. Korea* **2015**, *51*, 53–66, doi:10.14770/jgsk.2015.51.1.53.

7. Egawa, K.; Hong, S.K.; Lee, H.; Choi, T.; Lee, M.K.; Kang, J.G.; Yoo, K.-C.; Kim, J.C.; Lee, Y. I; Kihm, J.-H. Preliminary evaluation of geological storage capacity of carbon dioxide in sandstones of the Sindong Group, Gyeongsang Basin (Cretaceous). *J. Geol. Soc. Korea* **2009**, *45*, 463–472.

8. Wang, S.; Kim, J.; Lee, M. Measurement of the $scCO_2$ Storage Ratio for the CO_2 Reservoir Rocks in Korea. *In Proceedings of the Energy Procedia* **2016**, *97*, 342–347, doi:10.1016/j.egypro.2016.10.015.

9. Kim, S.; Kim, J.; Lee, M.; Wang, S. Evaluation of the CO_2 Storage Capacity by the Measurement of the $scCO_2$ Displacement Efficiency for the Sandstone and the Conglomerate in Janggi Basin. *Econ. Environ. Geol.* **2016**, *49*, 469–477.

10. Bachu, S.; Bonijoly, D.; Bradshaw, J.; Burruss, R.; Holloway, S.; Christensen, N.P.; Mathiassen, O.M. CO_2 storage capacity estimation: Methodology and gaps. *Int. J. Greenh. Gas Control* **2007**, *1*, 430–443, doi:10.1016/S1750-5836(07)00086-2.

11. Lindeberg, E.; Vuillaume, J.F.; Ghaderi, A. Determination of the CO_2 storage capacity of the Utsira formation. *In Proceedings of the Energy Procedia* **2009**, *1*, 2777–2784, doi:10.1016/j.egypro.2009.02.049.

12. Kopp, A.; Class, H.; Helmig, R. Investigations on CO_2 storage capacity in saline aquifers. Part 1. Dimensional analysis of flow processes and reservoir characteristics. *Int. J. Greenh. Gas Control* **2009**, *3*, 263–276, doi:10.1016/j.egypro.2017.03.1605.

13. Pingping, S.; Xinwei, L.; Qiujie, L. Methodology for estimation of CO_2 storage capacity in reservoirs. *Pet. Explor. Dev.* **2009**, *36*, 216–220, doi:10.1016/S1876-3804(09)60121-X.

14. Goodman, A.; Hakala, A.; Bromhal, G.; Deel, D.; Rodosta, T.; Frailey, S.; Small, M.; Allen, D.; Romanov, V.; Fazio, J.; Huerta, N.; Mclntyre, D.; Kutchko, B.; Guthrie, G. U.S. DOE methodology for the development of geologic storage potential for carbon dioxide at the national and regional scale. *Int. J. Greenh. Gas Control* **2011**, *5*, 952–965, doi:10.1016/j.ijggc.2011.03.010.

15. Knopf, S.; May, F. Comparing Methods for the Estimation of CO_2 Storage Capacity in Saline Aquifers in Germany: Regional Aquifer Based vs. Structural Trap Based Assessments. *In Proceedings of the Energy Procedia* **2017**, *114*, 4710–4721, doi:10.1016/j.egypro.2017.03.1605.

16. Elenius, M.; Skurtveit, E.; Yarushina, V.; Baig, I.; Sundal, A.; Wangen, M.; Landschulze, K.; Kaufmann, R.; Choi, J.C.; Hellevang, H.; Podladchikov, Y.; Aavatsmark, I.; Gasda, S.E. Assessment of CO_2 storage capacity based on sparse data: Skade Formation. *Int. J. Greenh. Gas Control* **2018**, *79*, 252–271, doi:10.1016/j.ijggc.2018.09.004.

17. Doughty, C.; Pruess, K.; Benson, S.; Hovorka, S.D.; Knox, P.R.; Green, C.P. Capacity investigation of brine-bearing sands of the Frio formation for geologic sequestration of CO_2. *Lawrence Berkeley Natl. Lab.* **2001**, http://hdl.handle.net/2152/64418.

18. Zhou, Q.; Birkholzer, J.T.; Tsang, C.F.; Rutqvist, J. A method for quick assessment of CO_2 storage capacity in closed and semi-closed saline formations. *Int. J. Greenh. Gas Control* **2008**, *2*, 626–639, doi:10.1016/j.ijggc.2008.02.004.

19. NETL(National Energy Technology Laboratory) Carbon Sequestration Atlas of the United States and Canada. Annual Report. **2008.**

20. Tasianas, A.; Koukouzas, N. CO_2 storage capacity estimate in the lithology of the mesohellenic trough, Greece. *In Proceedings of the Energy Procedia* **2016**, *86*, 334–341, doi:10.1016/j.egypro.2016.01.034.

21. Kim, M.-C.; Gihm, Y.S.; Son, E.-Y.; Son, M.; Hwang, I.G.; Shinn, Y.J.; Choi, H. Assessment of the potential for geological storage of CO_2 based on its structural and sedimentologic characteristics in the Miocene Janggi Basin, SE Korea. *J. Geol. Soc. Korea* **2015**, *51*, 253–271, doi:10.14770/jgsk.2015.51.3.253.

22. An, J.; Lee, M.; Wang, S. Evaluation of the Sealing Capacity of the Supercritical CO_2 by the Measurement of Its Injection Pressure into the Tuff and the Mudstone in the Janggi Basin. *Econ. Environ. Geol.* **2017**, *50*, 303–311.

23. Gaus, I. Role and impact of CO_2-rock interactions during CO_2 storage in sedimentary rocks. *Int. J. Greenh. Gas Control* **2010**, *4*, 73–89, doi:10.1016/j.ijggc.2009.09.015.

24. Park, J.; Baek, K.; Lee, M.; Wang, S. Physical property changes of sandstones in Korea derived from the supercritical CO_2–sandstone–groundwater geochemical reaction under CO_2 sequestration condition. *Geosci. J.* **2015**, *19*, 313–324, doi:10.1007/s12303-014-0036-4.

434 25. Jun, Y.S.; Giammar, D.E.; Werth, C.J. Impacts of geochemical reactions on geologic carbon
435 sequestration. *Environ. Sci. Technol.* **2013**, *47*, 3–8, doi:10.1021/es3027133.

436 26. Park, J.; Baek, K.; Lee, M.; Chung, C.-W.; Wang, S. The Use of the Surface Roughness Value to Quantify
437 the Extent of Supercritical CO_2 Involved Geochemical Reaction at a CO_2 Sequestration Site. *Appl. Sci.*
438 **2017**, *7*, 572, doi:10.3390/app7060572.

439 27. IPCC. IPCC Special Report on Carbon Dioxide Capture and Storage. Prepared by Working Group III of
440 the Intergovernmental Panel on Climate Change. **2005**.

441 28. Bachu, S.; Gunter, W.D.; Perkins, E.H. Aquifer disposal of CO_2: Hydrodynamic and mineral trapping.
442 *Energy Convers. Manag.* **1994**, *35*, 269–279, doi: 10.1016/0196-8904(94)90060-4.

443 29. Wigand, M.; Carey, J.W.; Schütt, H.; Spangenberg, E.; Erzinger, J. Geochemical effects of CO_2
444 sequestration in sandstones under simulated in situ conditions of deep saline aquifers. *Appl.*
445 *Geochemistry* **2008**, *23*, 2735–2745, doi:10.1016/j.apgeochem.2008.06.006.

446 30. Zhao, J.; Lu, W.; Zhang, F.; Lu, C.; Du, J.; Zhu, R.; Sun, L. Evaluation of CO_2 solubility-trapping and
447 mineral-trapping in microbial-mediated CO_2 -brine-sandstone interaction. *Mar. Pollut. Bull.* **2014**, *85*,
448 78–85, doi:10.1016/j.marpolbul.2014.06.019.

449 31. Dawson, G.K.W.; Pearce, J.K.; Biddle, D.; Golding, S.D. Experimental mineral dissolution in Berea
450 Sandstone reacted with CO_2 or SO_2-CO_2 in NaCl brine under CO_2 sequestration conditions. *Chem. Geol.*
451 **2015**, *399*, 87–97, doi:10.1016/j.chemgeo.2014.10.005.

452 32. Mediato, J.F.; García-Crespo, J.; Izquierdo, E.; García-Lobón, J.L.; Ayala, C.; Pueyo, E.L.; Molinero, R.
453 Three-dimensional Reconstruction of the Caspe Geological Structure (Spain) for Evaluation as a
454 Potential CO_2 Storage Site. *In Proceedings of the Energy Procedia* **2017**, *114*, 4486–4493,
455 doi:10.1016/j.egypro.2017.03.1608.

456 33. Span, R.; Wagner, W. A new equation of state for carbon dioxide covering the fluid region from the
457 triple-point temperature to 1100 K at pressures up to 800 MPa. *J. Phys. Chem. Ref. Data* **1996**, *25*, 1509–
458 1596, doi:10.1063/1.555991.

459 34. Spycher, N.; Pruess, K. CO_2-H_2O mixtures in the geological sequestration of CO_2. II. Partitioning in
460 chloride brines at 12-100 °C and up to 600 bar. *Geochim. Cosmochim. Acta* **2005**, *69*, 3309–3320,
461 doi:10.1016/j.gca.2005.01.015.